JOURNAL OF VIROLOGY, Sept. 2006, p. 8362–8370 Vol. 80, No. 17
0022-538X/06/$08.00+0 doi:10.1128/JVI.00814-06

West Nile Virus 5′-Cap Structure Is Formed by Sequential Guanine N-7 and Ribose 2′-O Methylations by Nonstructural Protein 5

Debashish Ray,[1] Aaloki Shah,[1] Mark Tilgner,[1] Yi Guo,[1] Yiwei Zhao,[1] Hongping Dong,[1] Tia S. Deas,[2] Yangsheng Zhou,[2] Hongmin Li,[1,2] and Pei-Yong Shi[1,2]*

Wadsworth Center, New York State Department of Health,[1] and Department of Biomedical Sciences, University at Albany, State University of New York,[2] Albany, New York 12201

Received 20 April 2006/Accepted 20 June 2006

Many flaviviruses are globally important human pathogens. Their plus-strand RNA genome contains a 5′-cap structure that is methylated at the guanine N-7 and the ribose 2′-OH positions of the first transcribed nucleotide, adenine (m^7GpppAm). Using West Nile virus (WNV), we demonstrate, for the first time, that the nonstructural protein 5 (NS5) mediates both guanine N-7 and ribose 2′-O methylations and therefore is essential for flavivirus 5′-cap formation. We show that a recombinant full-length and a truncated NS5 protein containing the methyltransferase (MTase) domain methylates GpppA-capped and m^7GpppA-capped RNAs to m^7GpppAm-RNA, using *S*-adenosylmethionine as a methyl donor. Furthermore, methylation of GpppA-capped RNA sequentially yielded m^7GpppA- and m^7GpppAm-RNA products, indicating that guanine N-7 precedes ribose 2′-O methylation. Mutagenesis of a K_{61}-D_{146}-K_{182}-E_{218} tetrad conserved in other cellular and viral MTases suggests that NS5 requires distinct amino acids for its N-7 and 2′-O MTase activities. The entire K_{61}-D_{146}-K_{182}-E_{218} motif is essential for 2′-O MTase activity, whereas N-7 MTase activity requires only D_{146}. The other three amino acids facilitate, but are not essential for, guanine N-7 methylation. Amino acid substitutions within the K_{61}-D_{146}-K_{182}-E_{218} motif in a WNV luciferase-reporting replicon significantly reduced or abolished viral replication in cells. Additionally, the mutant MTase-mediated replication defect could not be *trans* complemented by a wild-type replicase complex. These findings demonstrate a critical role for the flavivirus MTase in viral reproduction and underscore this domain as a potential target for antiviral therapy.

Most eukaryotic and viral mRNAs possess a 5′ cap that is important for mRNA stability and efficient translation (11). The cap consists of an inverted guanosine, methylated at the N-7 position, linked to the first transcribed RNA nucleotide by a unique 5′-5′ triphosphate bridge (m^7GpppN; cap 0 structure) (32). The process of RNA capping generally consists of three steps, in which the 5′ triphosphate end of the nascent RNA transcript is first hydrolyzed to a 5′ diphosphate by an RNA triphosphatase, then capped with GMP by an RNA guanylyltransferase, and finally methylated at the N-7 position of guanine by an RNA guanine-methyltransferase (N-7 MTase) (13). Additionally, the first and second nucleotides of many cellular and viral mRNAs are further methylated at the ribose 2′-OH position by a nucleoside 2′-O MTase to form cap 1 (m^7GpppNm) and cap 2 (m^7GpppNmNm) structures, respectively (11). Both N-7 and 2′-O MTases use *S*-adenosyl-L-methionine (AdoMet) as a methyl donor and generate *S*-adenosyl-L-homocysteine (AdoHcy) as a by-product. The order of the capping and methylation steps is variable among cellular and viral RNAs (11).

Many members of the *Flavivirus* genus are arthropod-borne human pathogens, including *West Nile virus* (WNV), *Yellow fever virus*, four serotypes of *Dengue virus* (DENV), *Japanese encephalitis virus*, *St. Louis encephalitis virus*, *Murray Valley encephalitis virus*, and *Tick-borne encephalitis virus* (4). The flavivirus genome is a single-stranded, plus-sense RNA of about 11,000 nucleotides that contains a type 1 cap at its 5′ end (5, 35) and terminates with 5′-CU_{OH}-3′ (35) (see Fig. 1A). 5′ and 3′ untranslated regions flank a single open reading frame which encodes a polyprotein that is co- and posttranslationally processed by viral and cellular proteases into three structural proteins (capsid [C], premembrane [prM] or membrane [M], and envelope [E]) and seven nonstructural proteins (NS1, NS2A, NS2B, NS3, NS4A, NS4B, and NS5) (4). Since flaviviruses replicate in the cytoplasm, they are expected to encode their own capping enzymes, rather than to use the host's capping apparatus located in the nucleus. Alternatively, since all host proteins have to be synthesized in the cytoplasm, it is possible that cellular capping components could be retained in the cytoplasm for viral RNA capping through specific interactions with a viral protein. Of the four enzymes required for flavivirus m^7GpppAm-cap formation, only the RNA triphosphatase and 2′-O MTase have been mapped to NS3 (19, 36) and NS5 (8), respectively, whereas the guanylyltransferase and N-7 MTase remain to be identified. The crystal structure of a ternary complex comprising the DENV-2 MTase domain, AdoHcy, and a GTP analogue suggested that, during 2′-O methylation, a specific cap-binding site holds the guanine cap to register the ribose 2′-OH of the first transcribed adenosine in close proximity to the AdoMet CH_3 donor (2, 8). Structure and sequence alignments of DENV, vaccinia virus VP39, and other 2′-O MTases indicate that a conserved K-D-K-E tetrad is positioned near the ribose 2′-OH group of the first transcribed nucleotide of the RNA substrate; this tetrad may participate in the 2′-O methyl transfer reaction (8). However, the N-7 MTase activity essential for flavivirus RNA cap formation

* Corresponding author. Mailing address: Wadsworth Center, New York State Department of Health, Albany, NY 12201. Phone: (518) 473-7487. Fax: (518) 473-1326. E-mail: ship@wadsworth.org.

has not been identified from biochemical or structural analyses of the DENV MTase (8).

Here we report that (i) the WNV full-length and the N-terminal NS5 MTase domain contain both N-7 and 2′-O MTase activities required for flavivirus 5′-cap formation; (ii) the two methylation events are sequential, with N-7 methylation preceding 2′-O methylation; (iii) the active sites of the two MTases share an essential D residue from the conserved K_{61}-D_{146}-K_{182}-E_{218} tetrad but likely require distinct residues for their individual activities; (iv) mutations that impair MTase activities significantly decrease or abolish flavivirus replication, possibly due to suboptimal viral translation from genomes containing unmethylated RNA cap; and (v) the defective replication mediated by the mutant MTase cannot be *trans* complemented in cells expressing a wild-type NS5 from a helper replicon.

MATERIALS AND METHODS

Cloning, expression, and purification of WNV NS5 and MTase domains. DNA fragments representing full-length NS5 and its N-terminal 300-amino-acid MTase domain were PCR amplified from an infectious WNV clone (29) and inserted into plasmid pET28(a) (Novagen) at NdeI and HindIII sites. A QuikChange II XL site-directed mutagenesis kit (Stratagene) was used to engineer an alanine substitution for K61, D146, K182, or E218 in the MTase domain. All constructs were verified by DNA sequencing. For protein expression, *Escherichia coli* strain Rosetta 2(DE3)pLysS (Novagen) bearing the expression plasmid was grown at 37°C to an absorbance of 0.8 at 600 nm, induced with 0.5 mM isopropyl-β-D-thiogalactopyranoside (IPTG) at 15°C for 12 h, and harvested by centrifugation. After sonication of the bacteria, soluble NS5 and MTase containing an N-terminal His tag were purified through a nickel-nitrilotriacetic acid column with an elution buffer containing 200 mM imidazole. The proteins (>90% purity) were further purified through a gel filtration 16/60 Superdex column (Amersham), analyzed by sodium dodecyl sulfate-polyacrylamide gel electrophoresis (SDS-PAGE), and quantified by Bradford protein assay (Bio-Rad).

Preparation of capped RNA substrates. RNA substrates representing the authentic 5′-terminal 190 nucleotides of the WNV genome were in vitro transcribed from PCR products generated using an infectious cDNA clone template (29) and primer I (5′-CAG*TAATACGACTCACTATTA*GTAGTTCGCCTGTG TGAGCTGACAAACTT-3′) and primer II (5′-TCTTCAGTCCAATCAAGGA CAACACGC-3′). A bacteriophage T7 class II ϕ2.5 promoter (italicized in primer I) was used to synthesize the ATP-initiated RNA (the underlined A in primer I) using T7 RNA polymerase (6). Capped RNAs were produced using m^7GpppA or GpppA cap analogues (New England Biolabs) at a 4:1 ratio relative to rATP, purified twice through Sephadex G-25 spin columns (Amersham), extracted with phenol-chloroform, and precipitated with ethanol. RNAs containing ^{32}P-labeled cap structures (m^7G*pppA or G*pppA) were prepared using a vaccinia virus capping enzyme following the manufacturer's protocol (Ambion), except that inorganic pyrophosphatase (0.004 unit) (US Biologicals) was added to enhance the yield of ^{32}P-labeled G*pppA-capped RNA (37). The m^7G*pppA-RNA or G*pppA-RNA was then purified as described for unlabeled transcripts.

MTase assays. The ^{3}H-methyl incorporation MTase assay (see Fig. 2C) was performed in a 20-μl reaction mixture containing 50 mM glycine, pH 10, 2 mM dithiothreitol, 80 μM unlabeled AdoMet (New England Biolabs), 2 μCi [^{3}H-methyl]AdoMet (Amersham), 10 pmol of m^7GpppA-RNA or GpppA-RNA substrate, and 30 pmol of WNV full-length NS5 or MTase protein. The reaction mixture was incubated at 22°C for 1 h. The resulting RNA was purified (described above), treated with nuclease P1 (see below) and alkaline phosphatase, and separated by thin-layer chromatography (TLC) on a polyethyleneimine cellulose plate. TLC slices containing the m^7GpppAm product (located between the m^7GpppA and GpppA bands) were quantified by scintillation counting.

The ^{32}P-labeled MTase assay was identical to the ^{3}H-methyl incorporation assay except that [^{3}H-methyl]AdoMet was omitted and 3×10^5 cpm of ^{32}P-labeled m^7G*pppA-RNA or G*pppA-RNA substrates was used. Control m^7G*pppAm-RNA was prepared by incubating the vaccinia virus VP39 protein in a 20-μl reaction mixture (containing 50 mM Tris-HCl, pH 8.0, 5 mM dithiothreitol, 10 μM AdoMet, 3×10^5 cpm of m^7G*pppA-RNA, and 30 pmol of recombinant VP39) for 1 h at 37°C. RNA cap structures were liberated with 5 μg of nuclease P1 (US Biologicals) in 10 mM Tris-Cl, pH 7.5, 1 mM $ZnCl_2$ or by tobacco acid pyrophosphatase (TAP) using conditions recommended by the manufacturer (Epicentre). The digestions (1 μl and 4 μl for ^{32}P- and ^{3}H-labeled assays, respectively) were spotted onto TLC plates and developed in 0.2 M (see Fig. 2B and 2C) or 0.3 M (see Fig. 2A, 3, 4, and 5) ammonium sulfate. The ^{32}P-labeled products were analyzed by autoradiography and quantified using a PhosphorImager.

Replicon analyses of MTase K-D-K-E tetrad and RNA cap structure. A *Renilla* luciferase (Rluc)-expressing replicon of WNV (21) was used to analyze the role of cap methylation in viral translation and RNA replication (RlucRep; see Fig. 6A). cDNAs of WNV RlucRep containing alanine substitutions for K61, D146, K182, or E218 of NS5 were prepared through PCR-mediated mutagenesis. Overlapping PCR fragments containing the targeted mutations were cloned into the AvrII sites at nucleotide positions 6316 and 8400 of the wild-type RlucRep (GenBank accession no. AF404756) (21). Mutations in the replicon plasmids were confirmed by sequencing. Replicon RNAs were transcribed using mMESSAGE mMACHINE kits (Ambion). The resulting RNAs (m^7GpppGA-RNA) contained an extra G (underlined) derived from the standard T7 promoter.

RlucReps containing various cap structures (m^7GpppAm, m^7GpppA, GpppA, or no cap [i.e., pppA]) were synthesized using MEGAscript kits (Ambion) in the presence of m^7GpppA, GpppA, or no cap analogues. The RlucRep with a 5′ m^7GpppAm was prepared by 2′-O methylation of the m^7GpppA-RlucRep RNA with WNV NS5. To eliminate the nonviral G residue derived from the standard T7 promoter, we transcribed the above replicons from a PCR product that contains a T7 ϕ2.5 promoter upstream of the RlucRep cDNA. To compare the translation and replication efficiencies of these replicons, we electroporated equal amounts of replicons (10 μg) into baby hamster kidney (BHK) cells and assayed for Rluc activities at indicated time points as previously described (21). For *trans*-complementation experiments, the same protocol was used to transfect replicon RNAs into BHK cells bearing the persistently replicating replicon expressing a neomycin phosphotransferase gene (28).

RESULTS

Expression and purification of full-length NS5 and MTase domain WNV. WNV NS5 consists of an N-terminal MTase and a C-terminal RNA-dependent RNA polymerase (RdRp) domain (14, 22) connected through a bridge domain containing a nuclear localization sequence (NLS) (Fig. 1A) (10). Full-length NS5 (905 amino acids) and the MTase (300 amino acids) proteins containing an N-terminal His tag were cloned, expressed, and purified to near-homogeneity through nickel-nitrilotriacetic acid affinity and gel filtration chromatography (Fig. 1B). SDS-PAGE analysis of the recombinant proteins showed the expected bands at 106 and 37 kDa for the full-length NS5 and MTase, with yields of about 5 mg and 8 mg per liter of bacterial culture, respectively.

NS5 methylates both the guanine N-7 and ribose 2′-O positions of the WNV RNA cap. Two types of capped RNA substrates (consisting of the authentic 5′-terminal 190 nucleotides of the WNV genome) were used to monitor N-7 and 2′-O MTase activities: m^7G*pppA-RNA (the asterisk indicates that the following phosphate is ^{32}P labeled) for detection of 2′-O methylation and G*pppA-RNA for detection of both N-7 and 2′-O methylations. Digestion of m^7G*pppA-RNA and G*pppA-RNA with nuclease P1 (which cleaves capped RNAs into 3′-OH-terminated cap structures and 5′-pN_{OH}) revealed two distinct bands on TLC plates (Fig. 2A, lanes 1 and 5). The bands were suggested to correspond to m^7G*pppA and G*pppA cap structures, based on their comigration with commercially available m^7GpppA and GpppA markers, respectively (data not shown). Remarkably, treatment of both RNA substrates with either full-length NS5 or the MTase domain of WNV in the presence of AdoMet resulted in products that comigrated with the m^7G*pppAm cap structure produced by

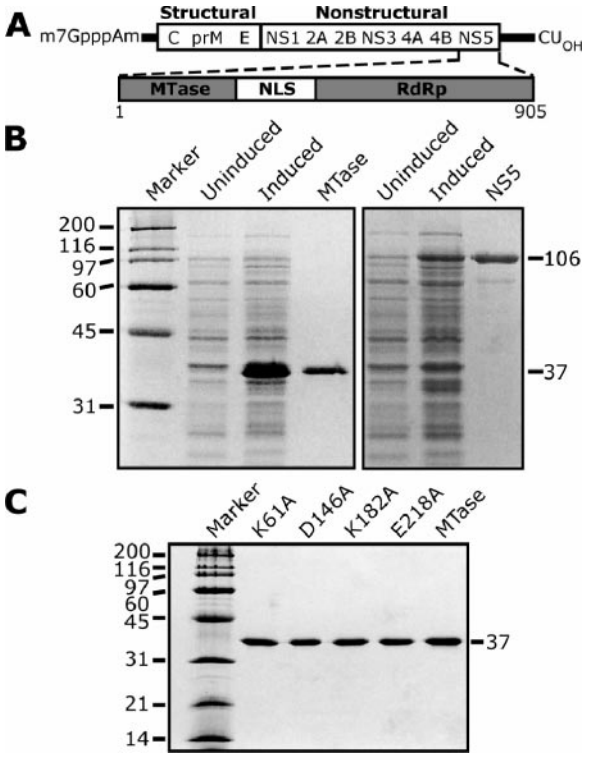

FIG. 1. Recombinant WNV NS5 and MTase proteins. (A) WNV genome. The 5′ and 3′ termini of the WNV genome contain an m^7GpppAm cap structure and CU_{OH}, respectively. The NS5 protein (905 amino acids) consists of the MTase and RdRp domains connected by a bridge domain harboring an NLS. (B) Purification of wild-type MTase and NS5 proteins. Uninduced and IPTG-induced bacteria and purified proteins were analyzed by SDS-PAGE and stained with Coomassie blue. (C) Mutant MTases each containing an alanine substitution within the conserved K_{61}-D_{146}-K_{182}-E_{218} tetrad. The sizes (kilodaltons) of protein standards (Marker) and recombinant proteins are indicated on the left and right, respectively.

vaccinia virus VP39 (Fig. 2A, compare lanes 2, 3, 6, and 7 with lane 4), a well-characterized m^7GpppA/G-dependent ribose 2′-O MTase (1). Alkaline phosphatase treatment and TLC analyses using different developing solvents (0.35 M $LiCl_2$ or 3.5 M urea) did not alter the migration pattern of the putative m^7G*pppAm cap structure (data not shown), indicating that the ^{32}P-labeled species are nuclease P1- and phosphatase-resistant cap structures and not ^{32}P-labeled artifacts. These results suggest that WNV NS5 and MTase domain contain both N-7 and 2′-O MTase activities.

The capped RNA substrates and products described above were also digested with TAP (which releases m^7G*p and G*p from m^7G*pppA- and G*pppA-capped RNAs, respectively [30]) to verify the N-7 MTase activity (Fig. 2B). As expected, TAP digestions of m^7G*pppA-RNA substrate treated with NS5, MTase, and VP39 yielded equal amounts of ^{32}P-labeled bands that comigrated with m^7G*p on TLC plates (Fig. 2B, lanes 1 to 4). In contrast, treatment of G*pppA-RNA with NS5 or MTase converted G*p to m^7G*p (Fig. 2B, lanes 5 to 7). These data confirmed that NS5 and MTase can methylate GpppA-RNA at the N-7 position of the guanine base.

Next, [^{3}H-methyl]AdoMet was used to monitor the extent of methylation of unlabeled m^7GpppA-RNA and GpppA-RNA substrates during the formation of m^7GpppAm-RNA (Fig. 2C). For both NS5 and MTase, the level of ^{3}H-methyl incorporation into GpppA-RNA was approximately 2.5-fold higher than that into m^7GpppA-RNA. This is consistent with the notion that NS5 and MTase mediate the transfer of two methyl groups onto GpppA-RNA (at N-7 and 2′-O positions), while only one methyl group is incorporated into m^7GpppA-RNA (at the 2′-O position). The results that both the MTase domain and full-length NS5 were active in the above assays suggest that the C-terminal RdRp and the bridge domains of NS5 are not required for the N-7 and 2′-O MTase activities.

WNV MTase does not methylate guanine N-7 and ribose 2′-OH of a nonviral RNA. To test if the sequence of RNA substrate is important for WNV MTase, we in vitro transcribed an RNA from plasmid pUC19 representing positions A574 to G763 (GenBank accession no. X02514). The plasmid RNA substrates were ^{32}P labeled in the same manner as WNV RNAs. No N-7 methylation activity was detected when plasmid G*pppA-RNA was used (Fig. 3, left panel). In contrast, WNV G*pppA-RNA was readily converted to m^7G*pppA-RNA. Similarly, the MTase could not perform 2′-O methylation on plasmid m^7G*pppA-RNA but could methylate WNV m^7G*pppA-RNA to m^7G*pppAm-RNA (Fig. 3, right panel). These results suggest that the WNV MTase requires viral sequence for both N-7 and 2-O methylations.

Sequential guanine N-7 and ribose 2′-O methylations of RNA cap structures. Kinetic analyses were performed to examine the order of cap methylation mediated by the WNV NS5. m^7G*pppA-RNA and G*pppA-RNA were methylated by full-length NS5 for various time periods, digested with nuclease P1, and analyzed by TLC. When m^7G*pppA-RNA substrate was methylated (Fig. 4A), an inverse relationship between the amounts of m^7G*pppA and m^7G*pppAm was observed, and 50% of the input m^7G*pppA was converted to m^7G*pppAm at about 22.5 min. When G*pppA-RNA substrate was used (Fig. 4B), m^7G*pppA was first detected at 1 min, reached a maximum at 5 min, and steadily declined at later time points, and 50% of the input G*pppA was converted to m^7G*pppA at about 3 min. Concurrently, the double-methylated m^7G*pppAm was first detected at 5 min and linearly increased until 60 min. Similar time course results were obtained when [^{3}H-methyl]AdoMet was used to methylate unlabeled m^7GpppA-RNA and GpppA-RNA substrates, followed by scintillation counting of TLC slices representing GpppA, m^7GpppA, and m^7GpppAm bands (data not shown). The observations that guanine N-7 methylation was detected first and that ribose 2′-O methylation was evident only after the accumulation of the N-7 methylated cap suggested a sequential methylation of RNA cap in the order of GpppA → m^7GpppA → m^7GpppAm.

Differential effects of the conserved K-D-K-E residues on N-7 and 2′-O methylation of RNA cap. Structure-based sequence alignment of various RNA MTases revealed a conserved K-D-K-E tetrad, which was shown to be the active site for the 2′-O MTase of vaccinia virus VP39 and RrmJ (a heat shock-induced 2′-O MTase) (3, 15, 25). To examine the role of the K-D-K-E motif in WNV N-7 and 2′-O MTase activities, we expressed and purified mutant MTase proteins each containing an alanine substitution for K61, D146, K182, or E218 (Fig. 1C).

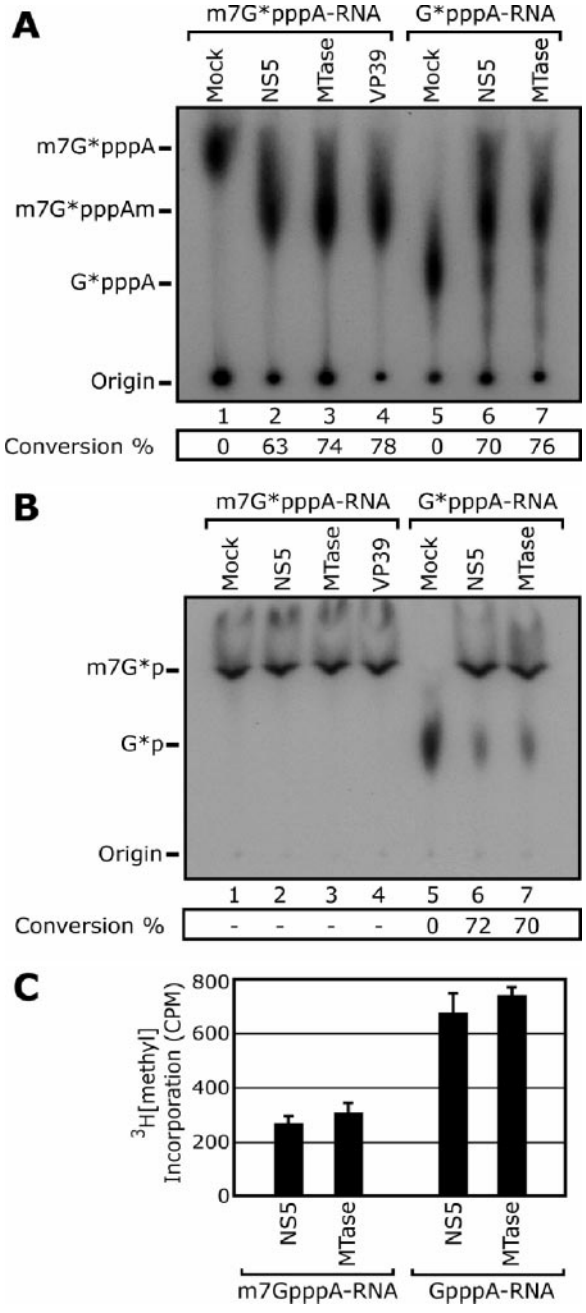

FIG. 2. Analyses of NS5- and MTase-generated cap structures. (A) TLC analysis of nuclease P1-resistant cap structures released from the WNV m^{7}G*pppA-RNA or G*pppA-RNA methylated with full-length NS5, MTase domain, VP39, or no protein (Mock). The asterisk indicates that the following phosphate is ^{32}P labeled. The positions of the origin and migration of G*pppA, m^{7}G*pppA, and m^{7}G*pppAm molecules are indicated on the left. The relative conversion from m^{7}G*pppA-RNA to m^{7}G*pppAm-RNA (lanes 2 to 4) and the relative conversion from G*pppA-RNA to m^{7}G*pppAm-RNA (lanes 6 and 7) were quantified with a PhosphorImager and are indicated below the autoradiograph. (B) TLC analysis of tobacco acid pyrophosphatase-digested products from the reactions in panel A. The positions of the origin, m^{7}G*p, and G*p molecules are indicated on the left. (C) ^{3}H-methyl incorporation into m^{7}GpppA-RNA and GpppA-RNA to form m^{7}GpppAm-RNA. The indicated RNA substrates were treated with MTase or NS5 in the presence of [^{3}H-methyl]AdoMet, digested with nuclease P1, and analyzed by TLC. The m^{7}GpppAm products were excised from the TLC plate, and ^{3}H-methyl incorporation was measured by scintillation counting. All assays were performed with equal amounts of NS5 and MTase proteins (30 pmol). Average results from three independent experiments are presented.

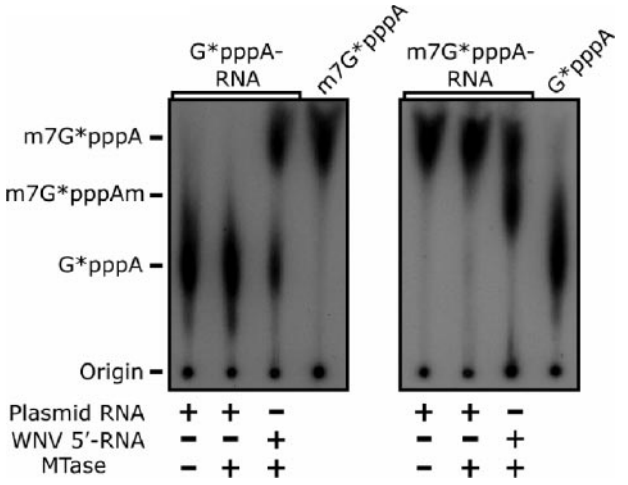

FIG. 3. WNV MTase requires a viral RNA sequence for N-7 and 2′-O methylations. RNA substrates representing positions A574 to G763 of plasmid pUC19 were prepared, treated with WNV MTase, digested with nuclease P1, and analyzed by TLC as described for WNV RNAs. WNV 5′-RNA substrates were included as positive controls. ^{32}P-labeled markers m^{7}G*pppA and G*pppA are indicated on top. (Right panel) G*pppA-RNA substrates were used to test N-7 MTase activity; the methylation reaction mixtures were incubated at room temperature for 5 min. (Left panel) m^{7}G*pppA-RNA substrates were tested for 2′-O MTase activity, and the methylation reaction mixtures were incubated for 1 h. Different incubation times were selected for the N-7 and 2′-O MTase reactions based on the methylation kinetics described in Fig. 4.

Analysis of the 2′-O MTase activity using m^{7}G*pppA-RNA substrate showed that each K-D-K-E mutation was lethal for 2′-O methylation (Fig. 5A). In contrast, when G*pppA-RNA substrate was used, N-7 MTase activity was completely abolished with the D146A mutation, whereas the quantities of m^{7}G*pppA products generated by the K61A, K182A, and E218A mutants were approximately 22%, 7%, and 16% of those produced by the wild-type MTase (Fig. 5B). These results suggest that (i) the conserved K-D-K-E residues form the active site for WNV 2′-O MTase and (ii) residue D146 is essential for both N-7 and 2′-O MTase activities, whereas the other three residues contribute to, but are not essential for, the N-7 MTase activity.

The conserved K-D-K-E tetrad of MTase is essential for WNV replication. An Rluc-expressing replicon of WNV (21) was used to analyze the role of cap methylation in viral translation and RNA replication (RlucRep, Fig. 6A). Transfection of BHK cells with RlucRep RNA was previously shown to yield two distinctive Rluc peaks, one at 2 to 10 h and the second after 24 h posttransfection (p.t.), representing viral translation and RNA replication of the transfected RlucRep, respectively (21, 34). The Rluc signals detected after 24 h p.t. correlated well with replicon synthesis levels and therefore could be used to indicate RNA replication (21, 33). An alanine substitution

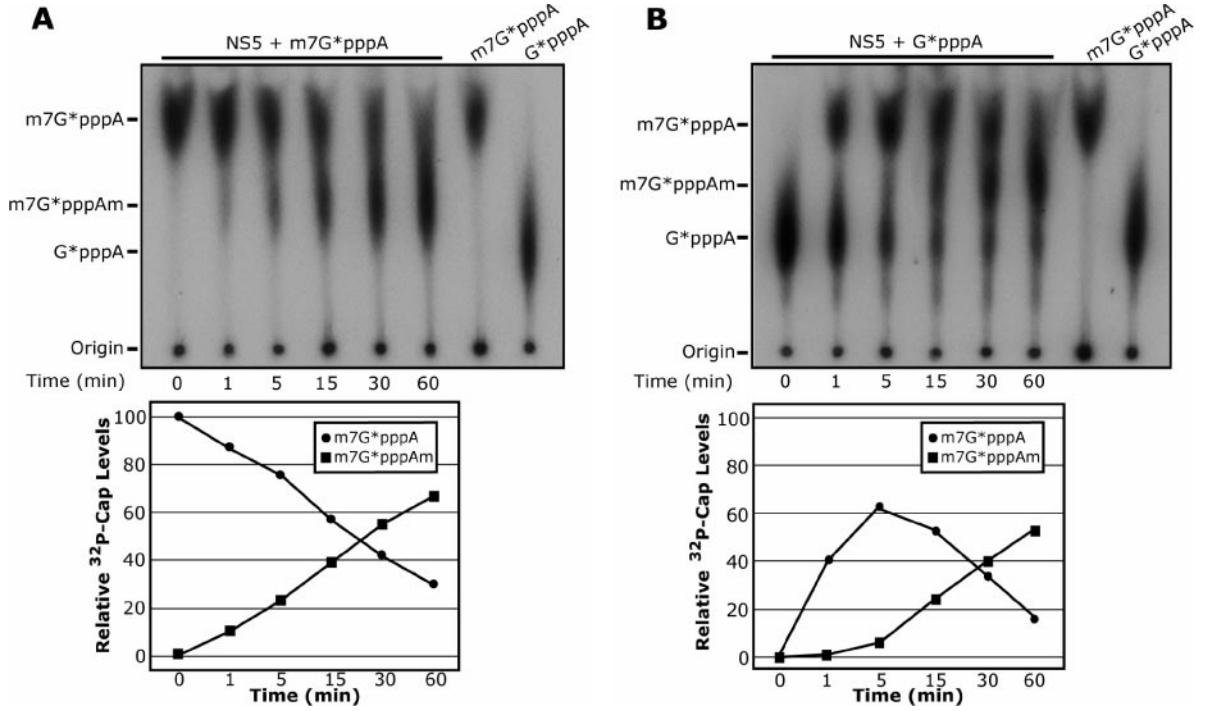

FIG. 4. Time course analyses of the NS5-mediated MTase activities. ^{32}P-labeled m^{7}G*pppA-RNA (A) and G*pppA-RNA (B) were methylated by full-length NS5 for the indicated times (minutes), digested with nuclease P1, and analyzed by TLC. ^{32}P-labeled markers m^{7}G*pppA and G*pppA are indicated on top. For each time point, the relative conversion from m^{7}G*pppA to m^{7}G*pppAm (A) and the relative conversion from G*pppA to m^{7}G*pppA and m^{7}G*pppAm (B) are presented below the autoradiograph. The input m^{7}G*pppA (0 min for A) or G*pppA (0 min for B) was set at 100%.

for K61, K182, D146, or E218 within the NS5 gene was engineered into the replicon. Equal amounts of wild-type and mutant RlucRep RNA, each of which was in vitro transcribed with an N-7 methylated cap structure, were transfected into BHK cells and assayed for the Rluc signals. At 2 h p.t., equal levels of Rluc activity were detected for the wild-type and mutant replicons, indicating similar levels of initial translation from input RNAs and similar transfection efficiencies (Fig. 6B, left panel). At 72 h p.t., the D146A and K182A replicons yielded a background level of Rluc signal (<0.05% of that generated by the wild-type replicon), suggesting that these two residues are essential for replicon replication (Fig. 6B, right panel); the K61A and E218A replicons produced Rluc activities of 1 to 2% of that of the wild-type replicon, suggesting that K61 and E218 are critical, but not essential, for replicon replication.

Mutations within the MTase active site cannot be *trans* complemented. Since the mutations within the K-D-K-E tetrad significantly impaired or completely abolished replicon replication, we examined whether the defective NS5 from the mutant replicons could be *trans* complemented by a wild-type NS5. Each mutant replicon (K61A, K182A, D146A, and E218A) was individually transfected into a stable BHK cell line that contained a persistently replicating WNV replicon expressing a neomycin phosphotransferase gene (NeoRep) (28). If the wild-type NS5 derived from the NeoRep could *trans* complement the K-D-K-E mutants, then the mutant replicon should have been able to replicate and therefore produce quantifiable Rluc signals. The results showed that, although similar levels of Rluc activities were observed at 2 h p.t., only the wild-type replicon yielded Rluc signals at 48 and 72 h p.t. (Fig. 6C and data not shown). These results demonstrated that point mutations within the MTase domain of WNV NS5 could not be *trans* complemented by wild-type replicase complexes. Our data agreed with a previous study of Kunjin virus showing that genomic RNAs containing deletions of greater than 75% of the C-terminal fragment of NS5 could not be *trans* complemented, whereas genomic RNAs containing deletions of less than 75% of the C-terminal fragment of NS5 could be *trans* complemented (18).

RNA cap structures modulate WNV RNA translation and replication. Replicon RNAs containing various cap structures (m^{7}GpppAm, m^{7}GpppA, GpppA, or no cap [i.e., pppA]) were transfected into BHK cells to directly measure the effects of RNA cap structure on WNV RNA translation (Fig. 7A). At 2 h p.t., the luciferase signals derived from uncapped pppA-RlucRep, unmethylated GpppA-RlucRep, and dimethylated m^{7}GpppAm-RlucRep were approximately 4%, 55%, and 99% of that derived from the monomethylated m^{7}GpppA-RlucRep, respectively (Fig. 7A, left panel). These results demonstrated that (i) the GpppA cap of the WNV replicon is critical for viral translation, (ii) N-7 methylation of the cap increases translation efficiency, and (iii) additional 2′-O methylation of the m^{7}GpppAm-RlucRep does not further improve viral translation. Interestingly, from 2 to 6 h p.t., the relative Rluc signal derived from GpppA-RlucRep consistently increased to about 73% of the signal derived from the m^{7}GpppA-RlucRep, whereas the relative Rluc levels for pppA-RlucRep and m^{7}GpppAm-RlucRep remained similar to the levels obtained

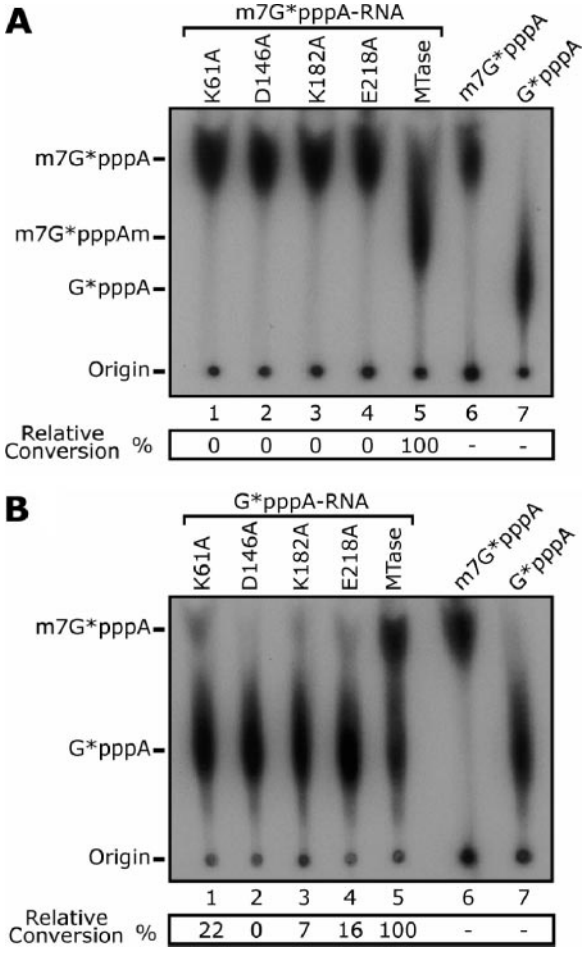

FIG. 5. Methylation activities of mutant MTases. Mutant MTases containing the indicated alanine substitutions were assayed for 2′-O MTase (A) and N-7 MTase activities (B) at 22°C for 1 h and 5 min, respectively. The shorter incubation time (5 min) was chosen for the N-7 MTase assay in panel B to minimize subsequent 2′-O methylation, which would complicate the quantification of the N-7-only methylated product (m^7GpppA). The experimental details were as described in Fig. 2. ^{32}P-labeled marker m^7G*pppA or G*pppA is indicated on top. The relative conversions for 2′-O methylation (m^7G*pppA to m^7G*pppAm in panel A) and for N-7 methylation (G*pppA to m^7G*pppA in panel B) were calculated by comparing the products produced from the mutant MTases with that generated from the wild-type protein (set at 100%).

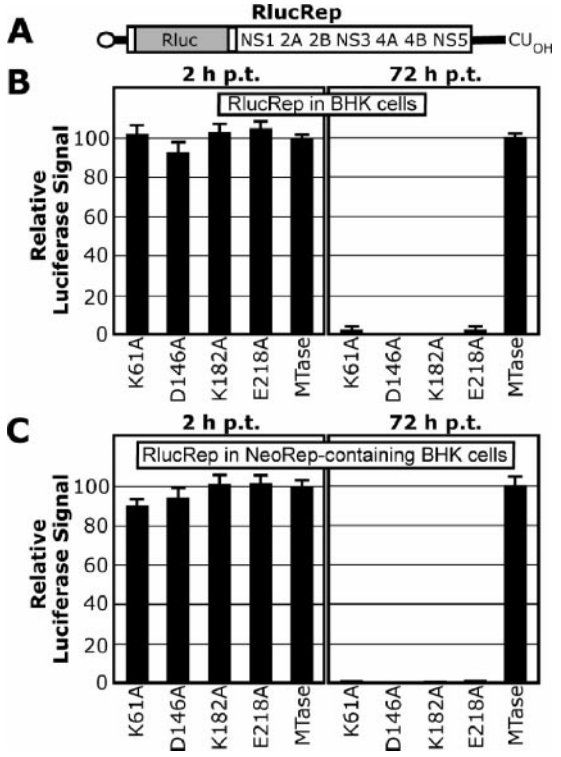

FIG. 6. Functional analyses of the effects of the conserved K_{61}-D_{146}-K_{182}-E_{218} tetrad on WNV translation and replication. (A) A luciferase-expressing WNV replicon. A *Renilla* luciferase reporter is fused in frame with the open reading frame of the genome at a position where viral structural genes were deleted, resulting in RlucRep. (B and C) RlucRep containing alanine substitutions for residues of the K_{61}-D_{146}-K_{182}-E_{218} tetrad was transfected into BHK cells (B) or into BHK cells that contained persistently replicating WNV replicon expressing a neomycin phosphotransferase gene (28) (C). At indicated time points, the transfected cells were lysed and quantified for luciferase activities. For each time point, luciferase signals derived from the wild-type RlucRep were set at 100%. For wild-type replicon, the luciferase signals collected at 72 h p.t. were consistently 80- to 100-fold higher than those collected at 2 h p.t., as previously described (34). Average results of three experiments are shown.

at 2 h p.t. (Fig. 7A, middle panel). The improved translation of input GpppA-RlucRep was most likely conferred by cap methylation of replicon mediated by the newly translated NS5. In line with the translation results, at 72 h p.t., replicon RNAs with m^7GpppAm, m^7GpppA, and GpppA caps exhibited a similar level of Rluc activity, whereas the uncapped pppA-RlucRep yielded only a background level of Rluc signal (Fig. 7A, right panel). These results suggested that defective translation and/or nuclease susceptibility of the uncapped pppA-RlucRep completely abolished its RNA replication. In contrast, the impaired translation of GpppA-RlucRep could be restored by the newly translated NS5 (probably through N-7 methylation), resulting in a high level of RNA replication.

To determine whether the low levels of viral translation and RNA synthesis from the uncapped pppA-RlucRep (Fig. 7A) were the result of template RNA degradation, we used an RdRp-defective RlucRep (21) to prepare RNAs with various capping structures (m^7GpppA-mt-RlucRep, GpppA-mt-RlucRep, and pppA-mt-RlucRep). The use of the replication-defective replicon allowed us to focus on viral RNA degradation without any complications derived from RNA replication. Equal amounts of replicon RNAs were electroporated into BHK cells, and real-time reverse transcription-PCR was performed to estimate the stability of the capped and uncapped viral RNAs (Fig. 7B). At 2 h p.t., similar amounts of viral RNA (about 3×10^7 copies per μg of extracted RNA) were detected for all three replicons. Surprisingly, all replicons were degraded in cells at a similar rate, as indicated by the percentage of viral RNA detected at 6, 12, and 20 h p.t. compared with that observed at 2 h p.t. (Fig. 7B). The results strongly suggest that the defective replication observed for the uncapped pppA-RlucRep is due to a significant loss of RNA translation, and not decreased stability.

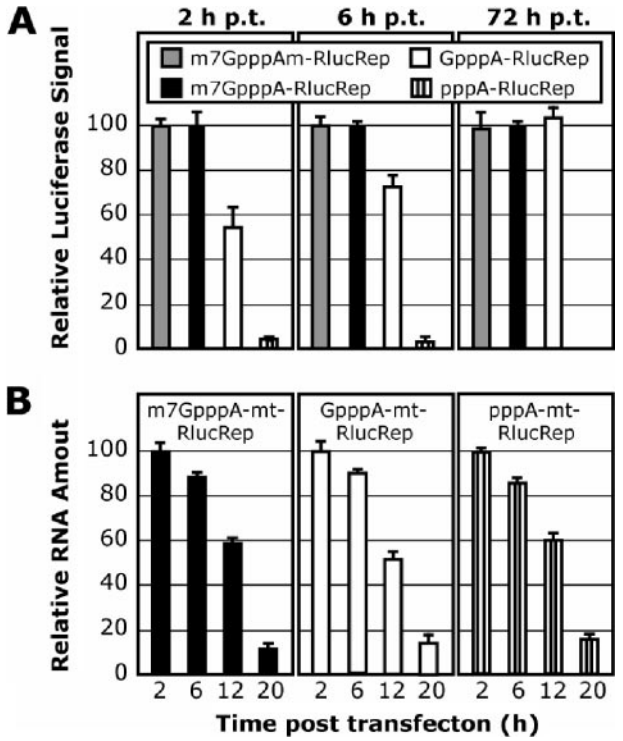

FIG. 7. Effects of RNA cap structures on WNV RNA translation, replication, and stability. (A) Analysis of the effect of 5′-cap structure on viral translation and replication. Wild-type RlucRep RNAs containing indicated cap structures were transfected into BHK cells, and luciferase activities were quantified at indicated time points. For each time point, luciferase signals derived from the m^7GpppA-RlucRep were set at 100%. (B) Analysis of the effect of 5′-cap structure on WNV RNA stability. A mutant RlucRep that contained a defective WNV polymerase (mt-RlucRep) (21) was used to prepare RNAs with indicated 5′-cap structures. The replicon RNAs (10 μg) were transfected into BHK cells. At 2, 6, 12, and 20 h p.t, a primer/probe set targeting WNV NS5 (27) was used to quantify viral RNA in real-time reverse transcription-PCR assays. For each replicon, the RNA level detected at 2 h p.t. was set at 100%. The degradation rate of RNA is indicated by the decrease in percentage of RNA level at later time points compared with the RNA level obtained at 2 h p.t. Average results of three experiments are shown.

DISCUSSION

Our results demonstrate that WNV NS5 sequentially catalyzes the guanine-N-7 and ribose 2′-O methylations involved in flavivirus RNA cap formation. Both MTase activities reside in the N-terminal portion of NS5 and do not require the downstream bridge and RdRp domains. In agreement with our results, the MTase domain of DENV-2 was reported to have 2′-O MTase activity; however, no N-7 MTase activity was observed (8). The latter discrepancy could have been caused by different assay conditions: we used an authentic RNA substrate representing the 5′-terminal 190 nucleotides of the WNV genome, whereas the DENV study used a short nonviral RNA substrate [GpppA$(C)_5$]. Interestingly, we found that a nonviral RNA of 190 nucleotides could not be methylated, highlighting the importance of viral sequence in cap methylation (Fig. 3). We also found that pH 10 was optimal for MTase activity (data not shown). The optimal methylation at high pH has also been reported for other MTases, such as DIM-5 (a histone H3 lysine 9 MTase) (38) and human guanine N-7 MTase (23). Nevertheless, our findings, together with the finding from a recent study that the C-terminal portion of WNV NS5 could function as an RdRp (26), suggest that flavivirus MTase and RdRp domains are functionally separable in vitro. Similarly, viruses in the order *Mononegavirales* were shown to contain functionally discrete cap-MTase and RdRp domains in a single L protein (7, 12, 23). In vesicular stomatitis virus, cap formation was found to be required for nonabortive RdRp-mediated viral mRNA transcription (12). Such coupling of cap formation and mRNA synthesis was executed by a specific transcriptase complex but not by a replicase complex (synthesizing uncapped genome-length RNA product) (24). Although the guanylyltransferase responsible for flavivirus capping remains to be identified, it would be interesting to test whether capping of the flavivirus genome is linked to viral RNA synthesis.

The suggestion that the WNV cap structure is formed through sequential methylations of the N-7 and 2′-O positions is supported by the following evidence. (i) Time course analysis of substrate GpppA-RNA showed an early accumulation of m^7GpppA-RNA, whose consumption coincided with increasing levels of dimethylated m^7GpppAm-RNA (Fig. 4B). (ii) No cap structure other than m^7GpppA and m^7GpppAm was detected throughout our assays. (iii) RNA substrate containing an N-7 methylated cap (m^7GpppA-RNA) could be directly converted to the dimethylated m^7GpppAm-RNA product (Fig. 4A). It is notable that neither of the two methylations converted all substrate to product under our assay conditions, including the 2′-O methylation mediated by the VP39 control (Fig. 2). This low efficiency of methylation was at least partially caused by the copurification of by-product AdoHcy (bound to the AdoMet-binding site) with the MTases (8, 17). Multiple rounds of dialysis of WNV NS5 (to remove the copurified AdoHcy) were found to improve the MTase activities (data not shown).

How does the WNV NS5 protein sequentially methylate the RNA cap at two separate positions? Structural alignment of AdoMet-dependent MTases showed that similarities are confined to the core MTase elements (which bind a single AdoMet molecule) among *Encephalitozoon cuniculi* (Ecm1) N-7 MTase (9), VP39 2′-O MTase (31), and DENV-2 MTase (8). Each of these MTases binds a single AdoMet molecule and utilizes it to catalyze the methyl transfer reaction. Therefore, it is conceivable that the AdoMet molecule located at the same binding site of the protein provides the methyl group for both N-7 and 2′-O methylations of WNV RNA cap. Structure superimposition of the DENV-2 MTase on the Ecm1 N-7 MTase-substrate complex indicated that no steric hindrance exists between the guanosine cap analogue and the DENV-2 MTase (data not shown), providing evidence of possible structural feasibility. Nevertheless, during the two methylations, the 5′ terminus of RNA should be repositioned as (i) the 2′-O and N-7 MTases have different methyl acceptors and (ii) the chemistry of the guanine-N-7 methylation reaction is distinct from that of ribose-2′-O methylation. The structure of Ecm1 N-7 MTase suggests an in-line mechanism of methyl transfer without direct contacts between the enzyme and either the attacking nucleophile N-7 atom of guanine, the methyl carbon of AdoMet, or the leaving group sulfur of AdoHcy, and catalysis of N-7 methylation is accomplished through close proximity and geometry

of the two substrates (9). In contrast, structural and mutagenesis studies of VP39 and RrmJ 2′-O MTase suggest an S_N2 reaction of methyl transfer. This mechanism first requires deprotonation of the target 2′-OH mediated by the conserved K-D-K-E active site. Then, the deprotonated 2′-O nucleophilically attacks the methyl moiety of AdoMet (forming the S_N2-like transition state) to accomplish the methyl transfer (15, 16). In agreement with the 2′-O MTase mechanism, mutations of the K-D-K-E residues of WNV MTase completely knocked out 2′-O methylation, suggesting that these residues form the active site of the 2′-O MTase (Fig. 5A). However, only the D146A mutation completely abolished N-7 MTase activity, while mutations of the other three residues reduced the N-7 methylation efficiency (Fig. 5B). These results, together with the differences in chemistry between the N-7 and 2′-O methylations (described above), suggest that flavivirus NS5 likely requires residues distinct from the 2′-O MTase active site for the N-7 methylation.

Why is residue D146 from the conserved K-D-K-E tetrad required for both N-7 and 2′-O MTase activities? One possible role for the conserved D residue is to interact with other active site residues distinct for 2′-O and N-7 MTase activities. The active site for the N-7 MTase remains to be identified. For RrmJ 2′-O MTase, the conserved D124 is proposed to accept the proton from K164 so that the later residue could deprotonate the 2′-OH to execute the S_N2 reaction-mediated methyl transfer (described above) (15). Alternatively, the essential role of the conserved D residue in both N-7 and 2′-O methylations could result from its critical interaction with the methyl donor AdoMet. Crystal structures of MTases (including DENV, VP39, and RrmJ) showed that the side chain of the D residue in the tetrad forms a hydrogen bond with the amine group of the AdoMet (8, 15, 16). Replacement of the side chain of this residue with that of alanine could impair the binding affinity or shift the position of the AdoMet molecule and, consequently, abolish both MTase activities. In support of (but not distinguishing between) the above two hypotheses, a mutation of the conserved D (amino acid 1762) of the K-D-K-E motif in vesicular stomatitis virus L protein was recently shown to abolish both N-7 and 2′-O MTase activities (20). Additionally, substitution of a different D (amino acid 1671, not within the conserved K-D-K-E tetrad) in the AdoMet-binding site of the L protein was also reported to destroy both N-7 and 2′-O MTase activities (12).

Mutagenesis using a luciferase-reporting replicon (RlucRep) showed that the conserved K-D-K-E tetrad is essential for WNV replication in cells (Fig. 6). The replication efficiency of the mutant replicon correlated with the MTase activities of the mutant enzymes. The K61A and E218A mutations that retained 22% and 16% of the wild-type N-7 MTase activity, respectively, exhibited replication efficiencies of 1 to 2% of the wild-type replicon, while the D146A and K182A mutations that contained 0% and 7% of the wild-type N-7 MTase activity showed no RNA replication (less than 0.05% of the wild-type level) (compare Fig. 5B with Fig. 6B). Translation from replicons containing various cap structures showed that, compared with the unmethylated GpppA-RNA, N-7 methylation (m^7GpppA-RNA) increased the translation level by approximately twofold, while additional 2′-O methylation did not further improve the RNA translation (Fig. 7A). Therefore, the replication defect of the K-D-K-E mutant replicons is likely due to inefficient N-7 methylation of RNA cap, which decreases viral translation and consequently debilitates RNA replication during the WNV reproductive cycle. Alternatively, RNA synthesis and 5′ capping could be coupled during flavivirus replication, and thus, defects in RNA capping (due to inactivation of MTase in this study) could result in suppression of RNA synthesis. More studies are needed to test the above hypothesis in the flavivirus system. Finally, we showed that the defective replication of the K-D-K-E mutant replicons cannot be complemented in *trans* by a wild-type replicase complex. These findings suggest flavivirus MTase as an attractive target for antiviral therapy. Since cellular cap formation is a nuclear event, it may be possible to design compounds that specifically inhibit the cytoplasmically associated flaviviruses by repressing viral MTase activities.

ACKNOWLEDGMENTS

We are grateful to Kiong Ho for providing recombinant VP39 protein, to Paul Masters for critical reading of the manuscript, and to Sue Moyer for helpful discussions. We thank the Molecular Genetics Core and the Cell Culture Facility at the Wadsworth Center for DNA sequencing and for maintenance of BHK cells, respectively.

The work was partially supported by contract AI25490 and grants AI061193 and AI065562 from NIH. D.R. is supported by a postdoctoral fellowship from the National Sciences and Engineering Research Council of Canada.

REFERENCES

1. **Barbosa, E., and B. Moss.** 1978. mRNA(nucleoside-2′-)-methyltransferase from vaccinia virus. Characteristics and substrate specificity. J. Biol. Chem. **253:**7698–7702.
2. **Benarroch, D., M. P. Egloff, L. Mulard, C. Guerreiro, J. L. Romette, and B. Canard.** 2004. A structural basis for the inhibition of the NS5 dengue virus mRNA 2′-O-methyltransferase domain by ribavirin 5′-triphosphate. J. Biol. Chem. **279:**35638–35643.
3. **Bujnicki, J. M., and L. Rychlewski.** 2001. Reassignment of specificities of two cap methyltransferase domains in the reovirus lambda 2 protein. Genome Biol. **2:**RESEARCH0038.
4. **Chambers, T. J., C. S. Hahn, R. Galler, and C. M. Rice.** 1990. Flavivirus genome organization, expression, and replication. Annu. Rev. Microbiol. **44:**649–688.
5. **Cleaves, G. R., and D. T. Dubin.** 1979. Methylation status of intracellular Dengue type 2 40S RNA. Virology **96:**159–165.
6. **Coleman, T. M., G. Wang, and F. Huang.** 2004. Superior 5′ homogeneity of RNA from ATP-initiated transcription under the T7 phi 2.5 promoter. Nucleic Acids Res. **32:**e14.
7. **Duprex, W. P., F. M. Collins, and B. K. Rima.** 2002. Modulating the function of the measles virus RNA-dependent RNA polymerase by insertion of green fluorescent protein into the open reading frame. J. Virol. **76:**7322–7328.
8. **Egloff, M. P., D. Benarroch, B. Selisko, J. L. Romette, and B. Canard.** 2002. An RNA cap (nucleoside-2′-O-)-methyltransferase in the flavivirus RNA polymerase NS5: crystal structure and functional characterization. EMBO J. **21:**2757–2768.
9. **Fabrega, C., S. Hausmann, V. Shen, S. Shuman, and C. D. Lima.** 2004. Structure and mechanism of mRNA cap (guanine-N7) methyltransferase. Mol. Cell **13:**77–89.
10. **Forwood, J. K., A. Brooks, L. J. Briggs, C. Y. Xiao, D. A. Jans, and S. G. Vasudevan.** 1999. The 37-amino-acid interdomain of dengue virus NS5 protein contains a functional NLS and inhibitory CK2 site. Biochem. Biophys. Res. Commun. **257:**731–737.
11. **Furuichi, Y., and A. J. Shatkin.** 2000. Viral and cellular mRNA capping: past and prospects. Adv. Virus Res. **55:**135–184.
12. **Grdzelishvili, V. Z., S. Smallwood, D. Tower, R. L. Hall, D. M. Hunt, and S. A. Moyer.** 2005. A single amino acid change in the L-polymerase protein of vesicular stomatitis virus completely abolishes viral mRNA cap methylation. J. Virol. **79:**7327–7337.
13. **Gu, M., and C. D. Lima.** 2005. Processing the message: structural insights into capping and decapping mRNA. Curr. Opin. Struct. Biol. **15:**99–106.
14. **Guyatt, K. J., E. G. Westaway, and A. A. Khromykh.** 2001. Expression and purification of enzymatically active recombinant RNA-dependent RNA polymerase (NS5) of the flavivirus Kunjin. J. Virol. Methods **92:**37–44.
15. **Hager, J., B. L. Staker, H. Bugl, and U. Jakob.** 2002. Active site in RrmJ, a heat shock-induced methyltransferase. J. Biol. Chem. **277:**41978–41986.

16. **Hodel, A. E., P. D. Gershon, and F. A. Quiocho.** 1998. Structural basis for sequence-nonspecific recognition of 5′-capped mRNA by a cap-modifying enzyme. Mol. Cell **1:**443–447.
17. **Hodel, A. E., P. D. Gershon, X. Shi, and F. A. Quiocho.** 1996. The 1.85 A structure of vaccinia protein VP39: a bifunctional enzyme that participates in the modification of both mRNA ends. Cell **85:**247–256.
18. **Khromykh, A. A., P. L. Sedlak, and E. G. Westaway.** 1999. *trans*-Complementation analysis of the flavivirus Kunjin ns5 gene reveals an essential role for translation of its N-terminal half in RNA replication. J. Virol. **73:**9247–9255.
19. **Li, H., S. Clum, S. You, K. E. Ebner, and R. Padmanabhan.** 1999. The serine protease and RNA-stimulated nucleoside triphosphatase and RNA helicase functional domains of dengue virus type 2 NS3 converge within a region of 20 amino acids. J. Virol. **73:**3108–3116.
20. **Li, J., E. C. Fontaine-Rodriguez, and S. P. Whelan.** 2005. Amino acid residues within conserved domain VI of the vesicular stomatitis virus large polymerase protein essential for mRNA cap methyltransferase activity. J. Virol. **79:**13373–13384.
21. **Lo, L., M. Tilgner, K. Bernard, and P.-Y. Shi.** 2003. Functional analysis of mosquito-borne flavivirus conserved sequence elements within 3′ untranslated region of West Nile virus using a reporting replicon that differentiates between viral translation and RNA replication. J. Virol. **77:**10004–10014.
22. **Nomaguchi, M., T. Teramoto, L. Yu, L. Markoff, and R. Padmanabhan.** 2004. Requirements for West Nile virus (−)- and (+)-strand subgenomic RNA synthesis in vitro by the viral RNA-dependent RNA polymerase expressed in Escherichia coli. J. Biol. Chem. **279:**12141–12151.
23. **Ogino, T., M. Kobayashi, M. Iwama, and K. Mizumoto.** 2005. Sendai virus RNA-dependent RNA polymerase L protein catalyzes cap methylation of virus-specific mRNA. J. Biol. Chem. **280:**4429–4435.
24. **Qanungo, K. R., D. Shaji, M. Mathur, and A. K. Banerjee.** 2004. Two RNA polymerase complexes from vesicular stomatitis virus-infected cells that carry out transcription and replication of genome RNA. Proc. Natl. Acad. Sci. USA **101:**5952–5957.
25. **Schnierle, B. S., P. D. Gershon, and B. Moss.** 1994. Mutational analysis of a multifunctional protein, with mRNA 5′ cap-specific (nucleoside-2′-O-)-methyltransferase and 3′-adenylyltransferase stimulatory activities, encoded by vaccinia virus. J. Biol. Chem. **269:**20700–20706.
26. **Selisko, B., H. Dutartre, J. Guillemot, C. Debarnot, D. Benarroch, A. Khromykh, P. Despres, M. Egloff, and B. Canard.** 19 April 2006, posting date. Comparative mechanistic studies of de novo RNA synthesis by flavivirus RNA-dependent RNA polymerases. Virology [Epub ahead of print.] doi: 10.1016/j.virol.2006.03.026.
27. **Shi, P. Y., E. B. Kauffman, P. Ren, A. Felton, J. H. Tai, A. P. Dupuis II, S. A. Jones, K. A. Ngo, D. C. Nicholas, J. Maffei, G. D. Ebel, K. A. Bernard, and L. D. Kramer.** 2001. High-throughput detection of West Nile virus RNA. J. Clin. Microbiol. **39:**1264–1271.
28. **Shi, P. Y., M. Tilgner, and M. K. Lo.** 2002. Construction and characterization of subgenomic replicons of New York strain of West Nile virus. Virology **296:**219–233.
29. **Shi, P. Y., M. Tilgner, M. K. Lo, K. A. Kent, and K. A. Bernard.** 2002. Infectious cDNA clone of the epidemic West Nile virus from New York City. J. Virol. **76:**5847–5856.
30. **Shinshi, H., M. Miwa, K. Kato, M. Noguchi, T. Matsushima, and T. Sugimura.** 1976. A novel phosphodiesterase from cultured tobacco cells. Biochemistry **15:**2185–2190.
31. **Shiryaev, S., B. Ratnikov, A. Chekanov, S. Sikora, D. Rozanov, A. Godzik, J. Wang, J. Smith, Z. Huang, I. Lindberg, M. Samuel, M. Diamond, and A. Strongin.** 2006. Cleavage targets and the D-arginine-based inhibitors of the West Nile virus NS3 processing proteinase. Biochem. J. **393:**503–511.
32. **Shuman, S.** 2001. Structure, mechanism, and evolution of the mRNA capping apparatus. Prog. Nucleic Acid Res. Mol. Biol. **66:**1–40.
33. **Tilgner, M., T. S. Deas, and P.-Y. Shi.** 2005. The flavivirus-conserved pentanucleotide in the 3′ stem-loop of the West Nile virus genome requires a specific sequence and structure for RNA synthesis, but not for viral translation. Virology **331:**375–386.
34. **Tilgner, M., and P. Y. Shi.** 2004. Structure and function of the 3′-terminal six nucleotides of the West Nile virus genome in viral replication. J. Virol. **78:**8159–8171.
35. **Wengler, G.** 1981. Terminal sequences of the genome and replicative-form RNA of the flavivirus West Nile virus: absence of poly(A) and possible role in RNA replication. Virology **113:**544–555.
36. **Wengler, G., and G. Wengler.** 1991. The carboxy-terminal part of the NS 3 protein of the West Nile flavivirus can be isolated as a soluble protein after proteolytic cleavage and represents an RNA-stimulated NTPase. Virology **184:**707–715.
37. **Wu, X., and L. A. Guarino.** 2003. *Autographa californica* nucleopolyhedrovirus *orf69* encodes an RNA cap (nucleoside-2′-*O*)-methyltransferase. J. Virol. **77:**3430–3440.
38. **Zhang, X., H. Tamaru, S. I. Khan, J. R. Horton, L. J. Keefe, E. U. Selker, and X. Cheng.** 2002. Structure of the Neurospora SET domain protein DIM-5, a histone H3 lysine methyltransferase. Cell **111:**117–127.